EXPLORING THERMOELECTRIC GENERATION OF ELECTRICAL ENERGY FROM EXHAUST GAS HEAT: AN EXPERIMENTAL STUDY

Dilek Özlem ESEN, Mesut KAYA, Sief Addeen Yacoub A SHABANEH*

Faculty of Technology, Department of Automotive Engineering, Kocaeli University,Turkiye

Corresponding author email addresses: s.t.saif.s.t@gmail.com

The global increase in energy demand has driven the automotive sector to rely heavily on fossil fuels, contributing to harmful greenhouse gas emissions. Recent advancements in exhaust gas recovery aim to enhance the efficiency of internal combustion engines, thereby reducing fossil fuel consumption and mitigating global warming. This study explores the potential of thermoelectric heat recovery systems in automotive applications, focusing on recovering heat from exhaust gases to generate electrical energy. A prototype exhaust system using 27 thermoelectric generators was developed, demonstrating its potential to improve fuel economy by converting waste heat into usable electricity. The study achieved a maximum current of 0.47 A, a voltage of 13.05 V, and 6 W of electrical power over a five-hour operation period. However, the system required a cooling load of 1.792 kW to maintain functionality, highlighting challenges in efficiency and integration.

Keywords: Thermoelectric generator, peltier, exhaust, cogeneration.

1. Introduction

This research aifigms to integrate thermoelectric generators (TEG) into automotive applications by converting waste heat from internal combustion engines (ICE) into electrical energy. This system provides a dual benefit: it harnesses waste heat and reduces greenhouse gas emissions.The increased use of vehicles has led to significant exhaust gas emissions. To address this, automotive manufacturers are focusing on improving ICE efficiency. Approximately 30% of the energy from fuel is utilized for propulsion, while 70% is lost through exhaust gases and the cooling system [1].In parallel with improving ICE efficiency, research has explored alternative fuels like biodiesel to address environmental concerns. Biodiesel offers a promising pathway to reduce the environmental impact of ICEs, with numerous studies highlighting its potential benefits. For instance, a comparative review evaluates the performance and emission characteristics of eucalyptus-biodiesel blends in diesel engines, demonstrating reduced CO, HC, and particulate emissions with performance metrics comparable to diesel at specific blend ratios, although NOx emissions slightly increase [2]. Another review emphasizes similar environmental advantages, such as reduced particulate matter, CO, and HC emissions, albeit with slight reductions in engine performance and increased NOx levels [3]. Experimental studies have further explored the role of antioxidant additives, such as in jamun biodiesel blends, which significantly reduce NOx emissions without compromising other parameters [4].Studies on juliflora biodiesel-diesel blends and investigations into optimizing engine operating parameters underscore biodiesel's potential to complement advancements in ICE technology through improved fuel stability and enhanced engine efficiency [5,6].

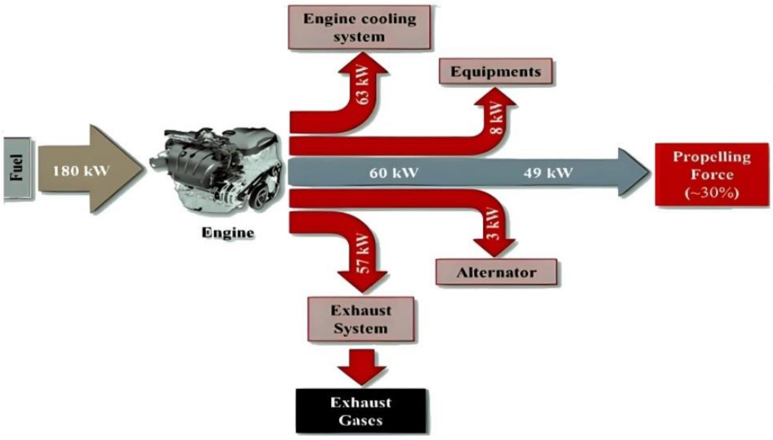

Figure 1. Distribution of energy obtained from fuel in the engine.

Building upon these advancements in alternative fuels, efforts to maximize energy recovery from ICEs have introduced cutting-edge technologies like TEGs. These systems aim to convert exhaust heat into usable energy, addressing inefficiencies in current energy systems while complementing the shift toward sustainable fuels. Although such technologies offer significant benefits, including enhanced energy recovery and reduced waste, the lack of experimental validation or detailed datasets limits the robustness of findings in some studies. For example, Yadav (2024) highlights the promise of these approaches but stresses the need for quantitative evaluations and real-world implementations to assess their scalability [7]. Similarly, Desai et al. (2024) investigate the performance of TEGs using a hybrid analytical and numerical approach, revealing valuable insights into optimizing waste heat recovery. However, the absence of experimental data and material innovations underscores the necessity for further research to strengthen their practical applicability and facilitate real-world integration [8]. This study examines the integration of a TEG with a gasoline engine to recover waste heat and improve overall energy efficiency. Experimental results highlight the TEG's capability to convert exhaust gas heat into electrical energy, with performance improving under higher engine loads and exhaust temperatures. Although the research effectively demonstrates TEG viability, it omits considerations of integration challenges and system durability, suggesting the need for further exploration of material optimization and long-term performance (Temizer et al., 2020) [9]. The research provides a thorough analysis of TEG systems for waste heat recovery, emphasizing the critical role of temperature gradients and material properties in enhancing energy and exergy efficiencies. While thermodynamic modeling offers valuable insights, the lack of experimental validation limits practical application, necessitating future empirical studies to explore innovative materials for real-world effectiveness (Ionescu, 2024) [10]. A novel approach using TEGs to convert heat from non-biodegradable dry waste into electricity shows potential for sustainable energy harvesting, though it overlooks environmental impacts and the need for cleaner materials (Lakshmi et al., 2024) [11]. The hybridization of TEGs with boiler exhaust systems improves energy recovery, but further research is required to address economic feasibility, durability, and scalability for industrial use (Farhat et al., 2024) [12]. Studies on TEGs in maritime applications and automotive exhaust systems demonstrate energy-saving potential but highlight the need for cost-effectiveness, long-term durability, and real-world implementation analyses (Perdana & Kusuma, 2023; Yoo & Rhi, 2023) [13,14].

Thermoelectric devices exploit the Seebeck effect to convert temperature differences into electrical energy. These devices comprise n- and p-type semiconductors, which are connected electrically in series, as illustrated in Tab. 2. The performance of these devices is primarily influenced by the properties of the junction materials and is quantified using a dimensionless figure of merit, denoted as ZT. This figure provides a comprehensive assessment of a thermoelectric material's electrical conversion efficiency [15]. The dimensionless figure of merit is expressed as:

$$ZT = \alpha^2 \sigma T / K \tag{1}$$

Here, α represents the Seebeck coefficient, σ denotes the electrical conductivity, and K signifies the thermal conductivity. These three transport parameters (α, σ, and K) are interdependent and influenced by various factors, including the band structure, carrier concentration, and other material properties . A higher figure of merit indicates superior performance of thermoelectric materials [16]. The ZT value is crucial in evaluating the efficiency of thermocouples and thermoelectric generators. A temperature gradient across the ends of an electrical conductor induces an electric voltage, the magnitude of which depends on the material properties. The Seebeck effect (α) is extensively utilized in temperature measurement through thermocouples and is gaining prominence in the conversion of waste heat into electrical energy via thermoelectric generators. The process is reversible; the reverse phenomenon, where voltage differences generate temperature differences, is known as the Peltier effect. In vehicles, the optimal locations for capturing excess heat from ICEs are the radiator and exhaust systems. The radiator prevents engine overheating and maintains optimal operating temperatures, while the exhaust system expels expanded exhaust gases[17].

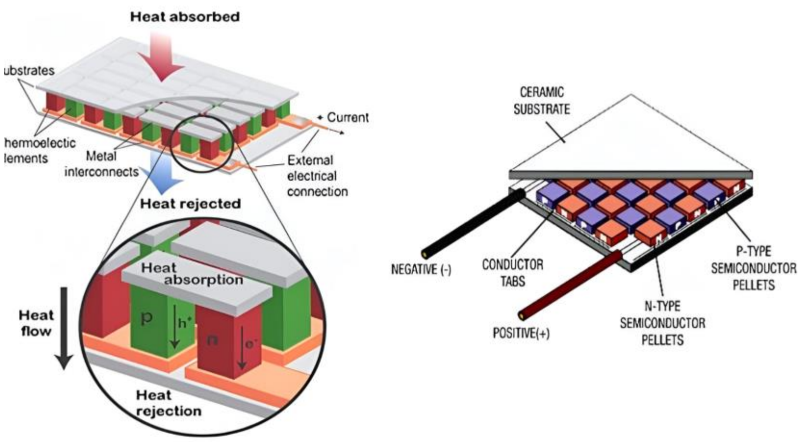

Figure 2. Schematic representation of p–n junctions in TEG devices

The internal energy of the waste heat from the exhaust is greater than that of the coolant circulating through the radiator. Zhang and Chau [18] noted that TEGs are predominantly installed in the exhaust system (exhaust manifold) due to its simplicity and minimal impact on engine operations. Furthermore, the high-temperature region of the exhaust manifold enhances the efficiency of the TEG system . An additional factor in maximizing the efficiency of waste heat recovery is the optimization of heat exchanger (HEX) geometry. M. Hatami et al. [19] analyzed various methods to increase heat transfer in HEXs and concluded that using fins is more effective than foams. They also found that a design with one inlet and two outlets improves the efficiency of the TEG system. X. Liu et al. [20] conducted similar studies on HEX design, aiming to enhance heat transfer from HEXs to Peltier modules, thereby improving the overall efficiency of exhaust heat recovery systems. Shengqiang Bai et al. [21] tested six different exhaust HEXs through numerical and experimental methods, finding that a structure with seven serial baffle plates transferred the maximum heat of 1737 W. Several studies have explored the application of TEGs in vehicles to increase efficiency and reduce fuel consumption. A summary of these studies, presented in Table 1, reveals that heat recovery efficiencies are low, both on a TEG basis (<3.5%) and a system basis (<2.5%). This highlights a significant challenge in using TEGs, primarily due to low thermal efficiency (typically $\eta_{th} < 4\%$) . As an auxiliary power source, Birholz et al. [22] installed a single TEG in a vehicle, generating 1 W of power. Bass et al. [23] developed a 1 kW TEG for diesel trucks through design and testing efforts. Matsubara [24] achieved a maximum power output of 266 W using newly designed TEGs on the exhaust pipe of a 2.0 L passenger vehicle. Crane et al. [25] tested a TEG system in a passenger vehicle, producing up to 700 W of power. Yang [26] reported the potential for generating 350 W in conventional trucks.

Table 1. Summary of thermoelectric power outputs, system efficiencies, and thermoelectric efficiencies from various experimental studies [26].

Ref.	**Year**	**Experimental Setup**	**Test Conditions**	**Element power output (W)**	**System efficiency (%)**	**Element efficiency (%)**
Takanose and Takamoshi [27]	1993	Gasoline 2 L engine	Tested from idling to 50-65 km/h hill climb	193 W	2.3	-
Ikoma et al. [28]	1999	Gasoline 2-3 L engine	60 km/h on 3-5% hill climb	130 W	1.1	2.9
Thacher et al. [29]	2007	5.8 L V8 gasoline engine	112.6 km/h, horizontal road	177 W	-	1.7
Schlichting et al. [30]	2008	Ninja 250R 2-cyl 248 cc	96.6 km/h freeway drive	0.47 W	-	-

2. Experimental Setup

The system, as shown in Fig. 3, was built at Kocaeli University Technical Education Faculty. This experimental setup simulates the exhaust system of a vehicle with an IC engine. It is designed to generate electricity using Peltier modules. A radiator system was incorporated to create a temperature difference between the hot and cold junctions, thereby protecting the Peltier modules from overheating.

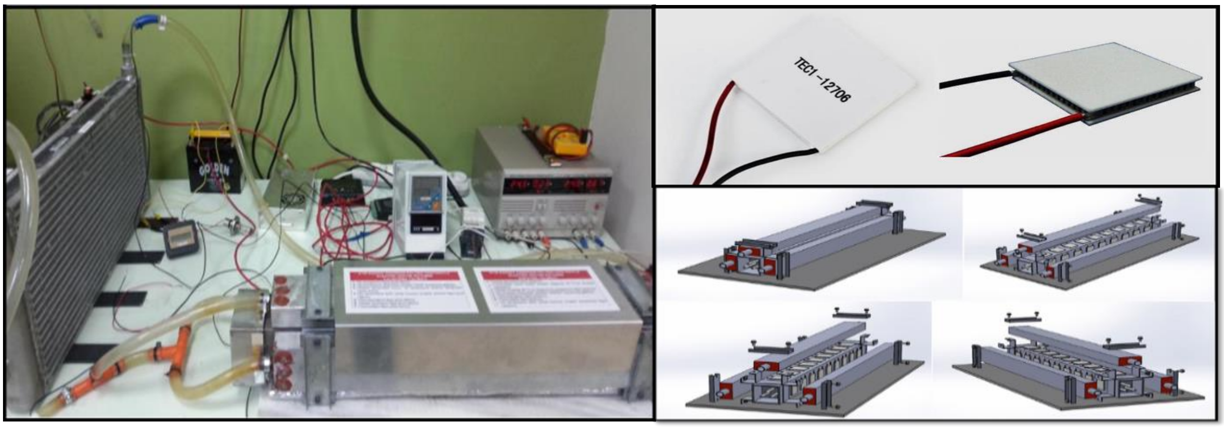

Figure 3. General view of the experimental setup, including a detailed view of the TEC 12706 module and the exhaust pipe with cooling blocks.

The system employs 27 TEC1-12706 TEGs to convert heat from the simulated exhaust pipe into electrical energy. A general view of the TEC1-12706 is provided in Fig. 3, and its specifications are detailed in Tab.2 an array of nine TEGs, stacked with thermal paste, are mounted on each side of the exhaust pipe simulation. Each array is connected in series, and these serial units are connected in parallel to one another. The hot junctions of the TEGs are placed on the heat source, i.e., the surface of the exhaust pipe, while the cold junctions are positioned on a heat sink. Three 600 W heaters are installed inside the exhaust pipe to simulate the heat of exhaust gas. A contactor and a thermo regulator control the heater temperatures, protecting the TEGs from excessive heat. The heater temperatures can be adjusted as needed to ensure safe operation. When the system is activated, a temperature difference is established between the hot and cold junctions, causing the TEGs on each side of the exhaust pipe to generate voltage and current. The voltage produced by the TEGs is recorded by a data logger and transferred to a computer, while the current is displayed on an ammeter. The energy generated from waste heat can be used to charge a 9 Ah battery.

Table 2. Specifications of the TEC1-12706 module [27].

Type	**Couples**	**Current (I_{max})**	**Voltage (U_{max})**	**Maximum cooling capacity Q_{max}(W)**	**Maximum temperature difference (between hot-**	**Reference temperature (at hot-end) T_h(K)**
TEC1-12706	127	6	15.2	56.5	68	300

A water pump circulates cooling water through the heat sinks. A mechanical flow meter, located at the pump's outlet, measures the flow rate of the cooling water. An expansion tank is placed between the radiator and the water pump to maintain a consistent flow rate. Additionally, two 12 V fans and a radiator are used to cool the coolant. The system incorporates five thermocouples to monitor temperatures at key points: the main inlet and outlet hoses of the heat sinks, the radiator water outlet, and the contacting surfaces of the hot and cold junctions in the upper array. These temperature readings are transmitted instantly via the thermocouples to a data logger, with the measurements stored on a computer. A separate data logger records the voltage generated by the TEGs.

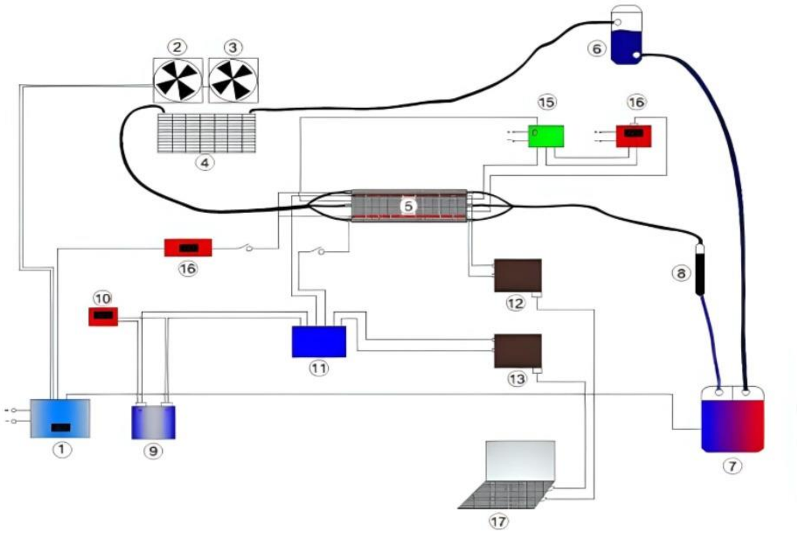

Figure 4. General structure of the experimental setup.

Table 3. Components of the experimental setup.

Item No	Name	Item No	Name
1	Power supply (12 V-24 V)	10	Battery indicator
2,3	Fan-1/2 (12 V)	11	Regulator
4	Radiator	12	Data logger-1 (temperature)
5	Exhaust pipe and cooling blocks	13	Data logger-2 (voltage)
6	Expansion tank	14	Thermoregulator
7	Water pump	15	Contactor
8	Flow meter (L/h)	16	Ampere meter
9	Battery (9 Ah)	17	Computer

2.1. Experimental Outputs

In the experiment, which generates electricity through TEGs, the coolant hoses are connected in series. As illustrated in Fig. 3, the coolant hose splits into three branches, each linked to a separate heat sink, before merging into a single main hose. After passing through each heat sink, the cooling water flows to the radiator via the main hose to dissipate the absorbed heat. The flow rate of the cooling water, measured by the flow meter at the water pump's outlet, is 500 L/h. Converting this to kg/s yields a flow rate of 0.139 kg/s, a crucial parameter for calculating the required cooling load. The temperatures of the hot and cold junctions, the temperature difference between them, and the inlet and outlet temperatures of the heat sinks and radiator are recorded by a data logger and summarized below.

Table 4. Temperature Data

Time	T_C (°C)	T_H (°C)	ΔT_J	Heat Sink Inlet	Heat Sink Outlet	Radiator Outlet
16:00:00	41.6	97.5	55.9	27.9	28.1	25.2
16:30:00	41.9	97.3	55.4	27.9	28.3	25.3
17:00:00	42.5	99.6	57.1	28.3	28.6	25.6
17:30:00	42.2	98.1	55.9	28.2	28.5	25.5
18:00:00	42.7	99.5	56.8	28.3	28.5	25.5
18:30:00	42.1	98.5	56.4	28.6	28.9	25.7
19:00:00	42.5	98.6	56.1	28.3	28.5	25.4
19:30:00	41.6	98.1	56.5	27.8	28.0	25.0
20:00:00	41.6	98.8	57.2	27.3	27.5	24.4
20:30:00	41.9	99.1	57.2	27.1	27.3	24.2
21:00:00	41.6	99.0	57.4	27.0	27.1	24.0

The relations between T_h&T_c values; voltage, current and power which are produced by the peltiers in the system are shown in below:

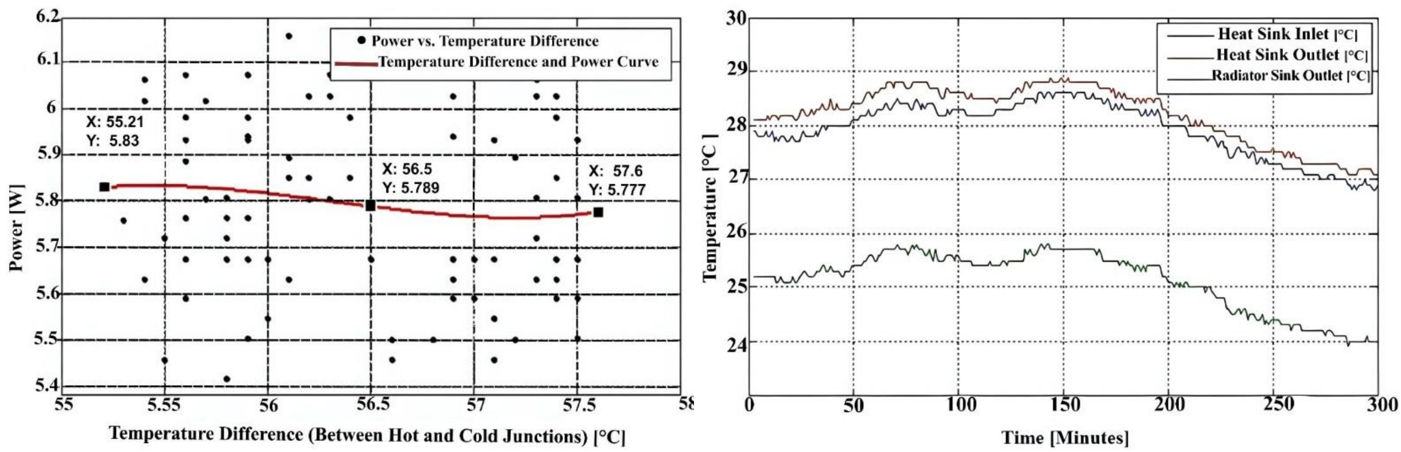

Figure 5.(a) Temperature difference between the hot and cold junctions and corresponding power production; (b) Coolant temperature variations.

As shown, the temperature difference between the hot and cold junctions aerages around 56.5°C. The power generated by the Peltier modules varied between 5.77 W and 5.83 W. Coolant water temperature differences during the experiment are depicted in Fig. 5. The temperature difference between the heat sink inlet and outlet is approximately 0.3°C. The water, which absorbs heat from the exhaust pipe, cools to about 25.1°C inside the radiator. The maximum temperature measured at the cold junction using a thermocouple was 43°C, while the coolant's maximum temperature reached 28.9°C. The maximum temperature difference between the hot and cold junctions was 57.7°C. During the experiment, the Peltier modules generated an average of 5.8 W of electrical energy, driven by the temperature differential between the hot and cold sides.

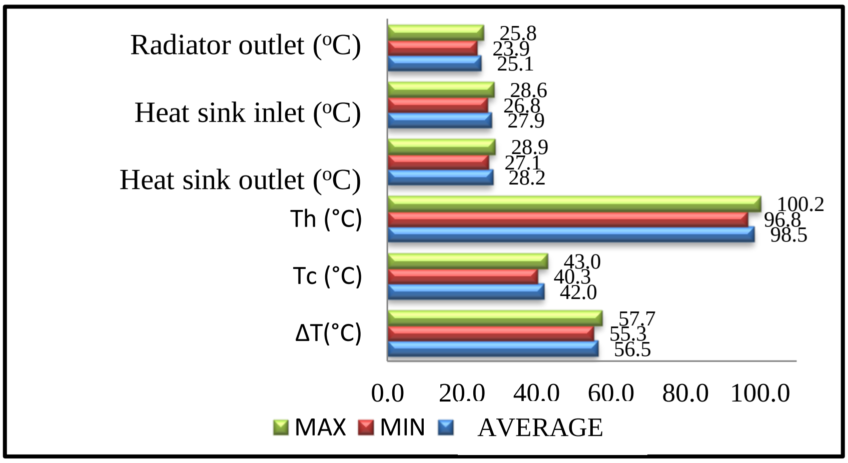

Figure 6. Radiator outlet temperature, heat sink inlet/outlet temperatures, T_h **,** T_c **and temperature difference** ΔT **data logger are analyzed.**

Table 5. Electrical outputs of the system.

Time	Ampere (A)	Voltage (V)	Power (W)
16:00:00	**0.43**	**12.8**	**5.504**
16:30:00	**0.45**	**12.9**	**5.805**
17:00:00	**0.46**	**12.9**	**5.934**
17:30:00	**0.44**	**12.9**	**5.676**
18:00:00	**0.43**	**13.0**	**5.590**
18:30:00	**0.46**	**13.0**	**5.980**
19:00:00	**0.46**	**13.2**	**6.072**
19:30:00	**0.46**	**13.2**	**6.072**
20:00:00	**0.45**	**13.1**	**5.895**
20:30:00	**0.46**	**13.1**	**6.026**
21:00:00	**0.46**	**13.2**	**6.072**

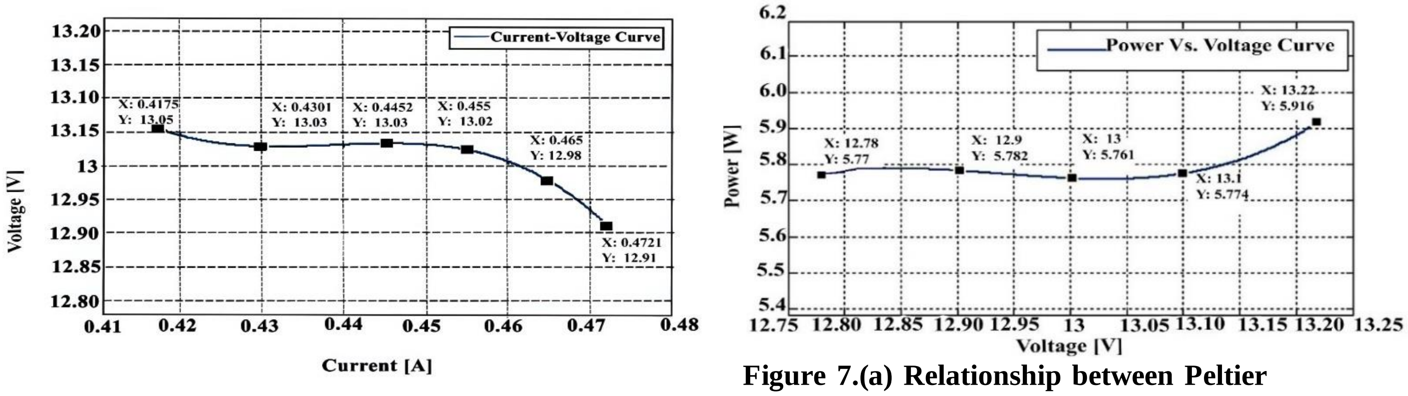

Figure 7.(a) Relationship between Peltier voltage and current, (b) Relationship between generated power and voltage.

The generated voltage, current, and power values are presented in Fig. 6. Detailed results indicate that the system produced an average voltage of 13.02 V and a current of 0.45 A. As seen in Fig. 7(a), the voltage generated by the TEGs varied between 12 V and 13 V during the experiment. When the current peaked at 0.4721 A, the voltage dropped to a minimum of 12.91 V. Fig. 7(b) shows the relationship between the voltage generated by the TEGs and the electrical power produced by the Peltier moduels.

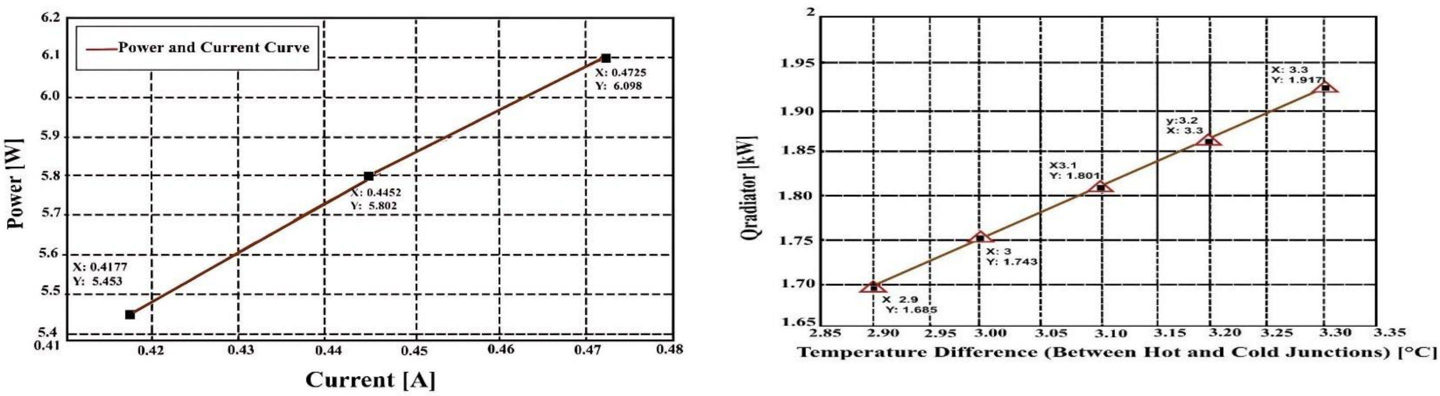

Figure 8. (a) Relationship between generated power and current, (b) Relationship between radiator heat load $Q_{radiator}$ and the temperature difference between radiator inlet and outlet

Fig. 8(a) illustrates the correlation between system current and electrical power generated by the Peltier devices, highlighting a limitation in their ability to produce alternating current (AC). The findings also indicate a strong dependence of electricity generation on the figure of merit. Fig. 8(b) details the cooling load calculation, determined to be 1.792 kW, which would impose an additional demand on the engine if a Peltier system were integrated into a vehicle. To address this inefficiency, either the electrical power output must be increased or the cooling load reduced. Increasing electrical power output could involve adding more TEGs, potentially by designing the exhaust pipe with a hexagonal or octagonal shape to accommodate additional units. Efficiency improvements could also be achieved by maximizing the temperature difference between the hot and cold surfaces of the TEGs. However, achieving a temperature difference of 500°C to attain 10% efficiency is currently unfeasible with existing technology. Advances in material science are expected to enable such efficiency gains in the future.

2.2. Discussion

The results of this experimental study emphasize two key aspects: (1) the electrical energy generated by thermoelectric generators (TEGs) and (2) the heat required to cool the hot junctions. On average, the experiment demonstrated that the system produced 13.02 V of electricity and 0.45 A of current.

$$P_{TEG} = V_{TEG} . I_{sys} \tag{2}$$

Here, V_{TEG} represents the voltage produced by the TEGs, I_{sys} is the current generated by the TEG system, and P_{TEG} is the electrical power (in watts) generated by the TEGs. Using the data obtained, the thermal efficiency of the system, where electricity is generated via thermoelectric generators, can be calculated as follows:

$$\eta = \frac{P_{TEG}}{\dot{Q}_{rad}} \tag{3}$$

In this equation, represents the system's efficiency. The term denotes the electrical power generated by the TEGs, as calculated using Eq. (2). To calculate in Eq. (3), it is necessary to determine the energy required to cool the water in the radiator. The term refers to the energy (in watts) needed to dissipate the heat absorbed by the cooling fluid (water) from the TEGs, which can be calculated using Eq. (4):

$$\dot{Q}_{rad} = \dot{m} . c . \Delta T \tag{4}$$

Here, $\dot{m}$ is the water flow rate, c is the specific heat capacity of water [4.18 kJ/kg°C], and ΔT is the temperature difference of the water. Over a five-hour operation period, the TEGs generated an average power output of 5.8 W. Another critical finding concerns the heat required to cool the water flowing through the system, calculated using the fundamental equation above.

Incorporating TEGs into automotive systems offers both economic and environmental benefits. A detailed economic analysis reveals that while initial installation costs of TEGs may be high due to the material and manufacturing requirements, these costs can be offset by long-term fuel savings resulting from improved energy efficiency. For instance, reducing fuel consumption by even a small percentage can yield significant savings over a vehicle's lifetime. From an environmental perspective, the deployment of TEGs contributes to a measurable reduction in CO_2 emissions by recovering energy that would otherwise be wasted. Preliminary calculations indicate that for every liter of fuel saved through TEG implementation, approximately 2.3 kg of CO_2 emissions are avoided. Such benefits not only enhance the sustainability of the system but also align with global efforts to mitigate climate change. These findings underscore the necessity of integrating economic viability and environmental impact assessments into the evaluation framework for thermoelectric technologies.

3. Major Limitations of the Study

The TEG system faces several critical limitations that affect its practical application in automotive systems. First, it requires a substantial cooling load of 1.792 kilowatts to maintain optimal performance, which imposes a significant energy burden and complicates its integration into vehicles without compromising efficiency gains. Second, the system's electrical output, with a peak power of six watts, remains relatively low, emphasizing the need for efficiency improvements to enable wider practical applications. Additionally, the inherent thermal efficiency constraints of current thermoelectric materials hinder the system's ability to effectively convert waste heat into electrical energy. Integration into existing vehicle architectures poses further challenges, as it necessitates modifications to vehicle cooling systems or other subsystems, leading to additional energy and space requirements. Lastly, the prolonged recharge time required for a 9 Ah battery renders the system impractical for direct energy storage applications in its current form. These limitations highlight the need for advancements in thermoelectric material efficiency, system design optimization, and innovative cooling solutions to improve the feasibility and practicality of this technology in automotive applications.

4. Conclusion

This study highlights the challenges and potential of TEG systems in automotive applications. Generating an average of 5.8 watts of electrical power required a significant cooling load of 1.792 kilowatts, underscoring that the current cogeneration system is inadequate for standalone electricity production. Furthermore, although the system demonstrated the capability to recharge a 9 Ah battery in approximately seven hours, this duration is impractical for real-world use. A more effective approach would be to utilize the generated electricity directly for auxiliary functions, such as interior vehicle lighting. The findings indicate that the current design of the Peltier system is inefficient. However, integrating the TEGs with the vehicle's existing cooling infrastructure, rather than constructing a separate cooling system, could provide a practical solution. This approach could enable more efficient recovery of waste heat to supplement the vehicle's electrical systems. Future advancements in thermoelectric material performance and system integration are crucial to fully unlocking the potential of this technology in automotive applications.

Nomenclature

A	- Ampere [A]	ΔT	- Temperature difference [°C]
Ah	- Ampere-hour	ΔT_j	- Temperature difference between hot &cold junction [°C]
T_c	- Cold junction temperature [°C]	K	- Thermal conductivity [W/m.K]
$\dot{Q}_{rad}$	- Cooling load [kW]	**V**	- Voltage [V]
Z	- Figure of merit	**W**	- Watt [W]
$\dot{m}$	- Flow rate [kg/sec]		
kg/s	- Flow rate unit [kg/sec]	**Greek symbols**	
L/h	- Flow rate unit [Liter/hour]	σ	- Electrical conductivity [S/m]
T_h	- Hot junction temperature [°C]	α	- Seeback coefficient [V/K]
ZT	- Non-dimensional figure of merit	η_{th}	- Thermal efficiency
P_{TEG}	- Power produced by TEG [W]	**Abbreviations**	
c	- Specific heat [kJ/kg.°C]	**HEX**	- Heat Exchanger
I_{sys}	- System current [A]	**ICE**	- Internal Combustion Engine
V_{TEG}	- TEG voltage[V]	**TEG**	- Thermoelectric Generator

References

[1] Hsiao Y.Y., Chang W.C., Chen S.L., A Mathematic Model of Thermoelectric Module with Applications on Waste Heat Recovery from Automobile Engine, *Energy, 35* (2010), 3, pp. 1447-1454. DOI No. 10.1016/j.energy.2009.11.030

[2] Ellappan, S., & Rajendran, S., A Comparative Review of Performance and Emission Characteristics of Diesel Engine Using Eucalyptus-Biodiesel Blend, *Fuel, 284* (2021), pp. 118925. DOI No. 10.1016/j.fuel.2020.118925

[3] Rajendran, S., A Comparative Study of Performance and Emission Characteristics of Neat Biodiesel Operated Diesel Engine: A Review, *Journal of Thermal Analysis and Calorimetry*, *146* (2021), 3, pp. 1015–1025. DOI No. 10.1007/s10973-020-10121-2

[4] Rajendran, S., & Ganesan, P., Experimental Investigations of Diesel Engine Emissions and Combustion Behaviour Using Addition of Antioxidant Additives to Jamun Biodiesel Blend, *Fuel*, *285* (2021), pp. 119157. DOI No. 10.1016/j.fuel.2020.119157

[5] Rajendran, S., Ganesan, P. & Anandkumar, G., A Comparative Assessment on Performance, Combustion and Emission Characteristics of Diesel Engine Fuelled by Juliflora Biodiesel-Diesel Blends, *Australian Journal of Mechanical Engineering*, *21* (2023), 1, pp. 257–269. DOI No. 10.1080/14484846.2020.1842294

[6] Ramalingam, S., Rajendran, S., Ganesan, P., & Govindasamy, M., Effect of Operating Parameters and Antioxidant Additives with Biodiesels to Improve the Performance and Reducing the Emissions in a Compression Ignition Engine – A Review, Renewable and Sustainable Energy Reviews, 81 (2018), Part 1, pp. 775–788. DOI No. 10.1016/j.rser.2017.08.026

[7] Yadav, A. K., Energy Generation from Exhaust Heat: Technologies and Innovations. *International Journal for Research in Applied Science and Engineering Technology*, *12* (2024), 7, pp. 854–859. DOI No. 10.22214/ijraset.2024.63654

[8] Desai, S., Dubey, S., & Gautham, M. G., Analytical and Numerical Approach for Performance Evaluation of Thermoelectric Generator. *Journal of Mines, Metals and Fuels*, *71* (2024), 12A, pp. 432–440. DOI No. 10.18311/jmmf/2023/43082

[9] Temizer, I., Yuksel, T., Can, I., & Alnak, D., Analysis of an Automotive Thermoelectric Generator on a Gasoline Engine. *Thermal Science*, *24*, (2020), (1 Part A), pp. 137–145. DOI No. 10.2298/TSCI180105096T

[10] Ionescu, V., Thermal, Energy and Exergy Analysis of Thermoelectric Generator System for Waste Heat Recovery Applications. *Journal of Ecological Engineering*, *25* (2024), 7, pp. 201–211. DOI No. 10.12911/22998993/188274

[11] Lakshmi, P. V., Sumalatha, A., Rani, K. S., Kalyan, K., Sekhar, O. C., & Sai Aasritha, K., Thermoelectric Energy Harvesting from Non-Biodegradable Dry Waste, *Proceedings*, 5th International Conference on Recent Trends in Computer Science and Technology (ICRTCST), Jamshedpur, India, 2024, pp. 472–475. DOI No. 10.1109/ICRTCST61793.2024.10578537

[12] Farhat, O., Khaled, M., Faraj, J., Hachem, F., & Castelain, C., Hybridization of heat recovery from exhaust gas of boilers using thermoelectric generators. Journal of Physics: Conference Series, Athens, Greece, 2024, Vol. 2754(1), pp. 012023. DOI No. 10.1088/1742-6596/2754/1/012023

[13] Perdana, Y. S., & Kusuma, C., Development of Thermoelectric Generator for Energy Saving Device Using Exhaust Waste Heat in Patrol Boat. *International Journal of Marine Engineering Innovation and Research*, *8* (2023), 3. DOI No. 10.12962/j25481479.v8i3.16249

[14] Yoo, J.-G., & Rhi, S.-H., Simulation Study on Thermoelectric Power Generation Using Waste Heat Recovery from Car Exhaust Gas, *Journal of Industrial Science and Technology Institute*, *37* (2023), 02, pp. 17–22. DOI No. 10.54726/JISTI.37.2.3

[15] Zhang, W., Weng, S., Luo, H., Li, G., Cai, Y., Gao, J., Zhang, F., & Yang, B., Experiments on Waste Heat Thermoelectric Generator for Power Transformer and its Field Application, *Journal of Physics: Conference Series*, Hangzhou, China, 2024, Vol. 2836(1), pp. 012022. DOI No. 10.1088/1742-6596/2836/1/012022

[16] Shen L., Xiao F., Chen H., Wang S., Investigation of a Novel Thermoelectric Radiant Air Conditioning System, *Energy and Buildings 59* (2013), pp. 123-132. DOI No. 10.1016/j.enbuild.2012.12.041

[17] R. Saidur, M. Rezaei, W.K. Muzammil, M.H. Hassan, S. Paria, M. Hasanuzzaman., Technologies to Recover Exhaust Heat From Internal Combustion Engines, *Renewable and Sustainable Energy Reviews*, *16* (2012), 8, pp. 5649-5659. DOI No. 10.1016/j.rser.2012.05.018

[18] Yang J., Potential Applications of Thermoelectric Waste Heat Recovery in the Automotive Industry, in international conference on thermoelectrics, Clemson, SC, USA, 2005, pp. 155-159. DOI No. 10.1109/ICT.2005.1519911

[19] Hatami M., Ganji DD., Gorji-Bandpy M., A Review of Different Heat Exchangers Designs for Increasing the Diesel Exhaust Waste Heat Recovery, *Renewable Sustainable Energy Reviews*, *37* (2014), pp. 168–181. DOI No. 10.1016/j.rser.2014.05.004

[20] X. Liu., Y.D. Deng., K. Zhang., M. Xu., Y. Xu., C.Q. Su., Experiments and Simulations on

Heat Exchangers in Thermoelectric Generator for Automotive Application, *Applied Thermal Engineering*, *71* (2014), 1, pp. 364-370. DOI No. 10.1016/j.applthermaleng.2014.07.022

[21] Crane D.T., Jackson G.S., Optimization of Cross Flow Heat Exchangers for Thermoelectric Waste Heat Recovery. *Energy Conversion and Management*, *1* (2014), pp. 26–35. DOI No. 10.1016/j.susmat.2014.11.002

[22] Bass JC., Elsner NB., Leavitt A., Performance of the 1 KW Thermoelectric Generator for Diesel Engines. In: Proceedings of the 13th international conference on thermoelectrics, New York, USA, 1995, Vol. 316, pp. 295–298. DOI No. 10.1063/1.46818

[23] Bass JC., Kushch AS., Elsner NB., Thermoelectric Generator (TEG) for Heavy Diesel Trucks. *Proceedings*, of the 10th international conference on thermoelectrics, Beijing, China, 2001, Vol. 4, pp. 422-430,

[24] Matsubara K., The Performance of a Segmented Thermoelectric Convertor Using Yb-Based Filled Skutterudites and Bi_2Te_3-Based Materials. In: MRS symposium proceedings, Warrendale, USA, 2002, Vol. 691. DOI No. 10.1557/PROC-691-G9.1

[25] Crane D., LaGrandeur J., Jovovic V., TEG on-Vehicle Performance and Model Validation and What it Means for Further TEG Development, *J Electron Mater*, *42* (2012), 7, pp. 1582–1591. DOI No. 10.1007/s11664-012-2327-8

[26] A. S. Kushch, J. C. Bass, S. Ghamaty and N. B. Eisner, Thermoelectric development at Hi-Z technology,*Proceedings, ICT2001*, 20 International Conference on Thermoelectrics, Beijing, China, 2001, pp. 422-430, DOI No. 10.1109/ICT.2001.979922

[27] Takanose E., Tamakoshi H., The Development of Thermoelectric Generator for Passenger Car, *Proceedings*, 12th IEEE international conference on thermoelectrics, Yokohama, Japan, 1993, pp. 467–470.

[28] Ikoma K., Munekiyo M., Furuya K., Kobayashi M., Izumi T., Shinnohara K., Thermoelectric Generator for Gasoline Engine Vehicles Using Bi_2Te_3 Modules, *J Japan Inst Metals*, *63* (1999), 11, pp. 1475–1478. DOI No. 10.2320/jinstmet1952.63.11_1475

[29] Thacher E., Helenbrook B., Karri M., Richter C., Testing of an Automobile Exhaust Thermoelectric Generator in a Light Truck. *Proc Inst Mech Eng D J Auto Eng*, *221* (2007), pp. 95–107. DOI No. 10.1243/09544070JAUTO51

[30] Schlichting A., Anton S., Inman D., Motorcycle Waste Heat Energy Harvesting, *Proceedings*, of the SPIE Industrial and Commercial Applications of Smart Structures Technologies, San Diego, California, United States, 2008. pp. 6930. DOI No. 10.1117/12.775783

Submitted: 28.10.2024.
DATE OF CORRECTED PAPER: 03.12.2024
DATE OF ACCEPTED PAPER: 11.02.2025.